

The University of Adelaide

School of Chemical Engineering

Cooperative Research Centre for Clean  
Power from Lignite

Physical Modelling of Mixing Between  
Rectangular Jets Present in Tangentially  
Fired Brown Coal Boilers

Ph.D. Thesis

Alessio Angelo Scarsella

## C.2. Transverse Flow Visualisation of the Secondary Jet

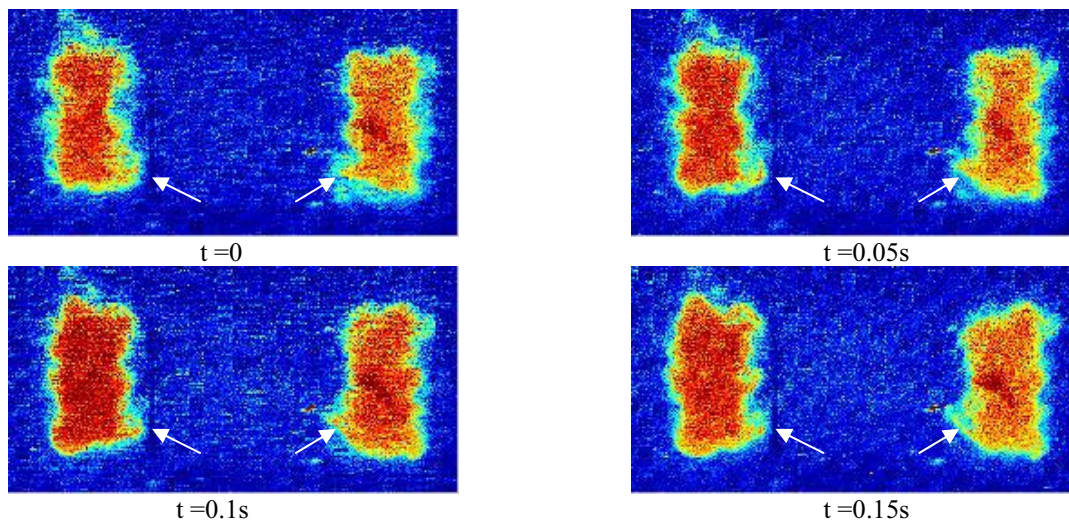


**Figure C. 31:** Instantaneous flow visualisation of the normalised concentration of the secondary jet at  $x/D=0.5$ , at 0.05 second intervals,  $\lambda = 0.55$ ,  $\gamma=0.3$ ,  $\kappa=0.18$ . The white arrows highlight the distortion of the secondary jets with an alteration in the local velocity gradients.

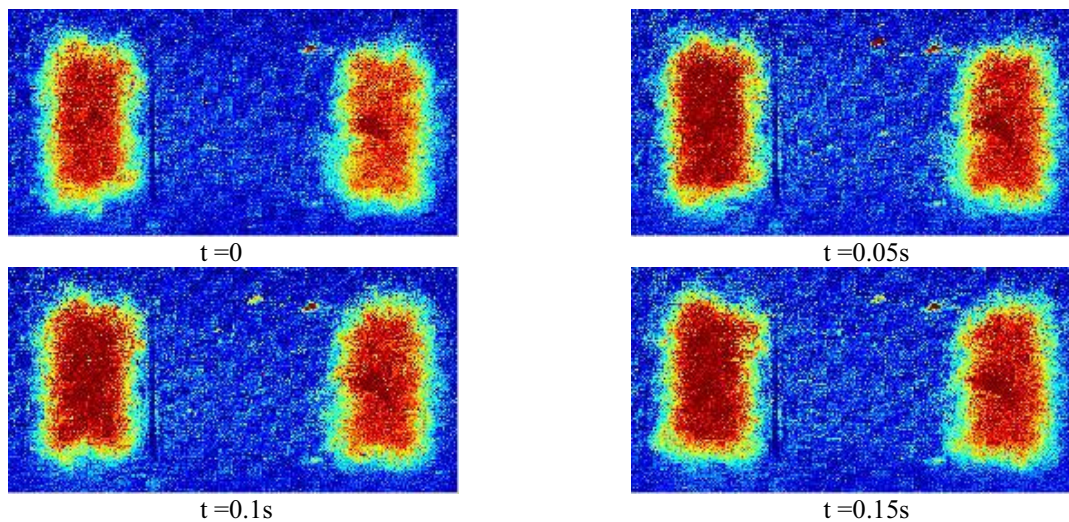


**Figure C. 32:** Instantaneous flow visualisation of the normalised concentration of the secondary jet at  $x/D=0.5$ , at 0.05 second intervals,  $\lambda = 1.4$ ,  $\gamma=1.96$ ,  $\kappa=1.18$ .

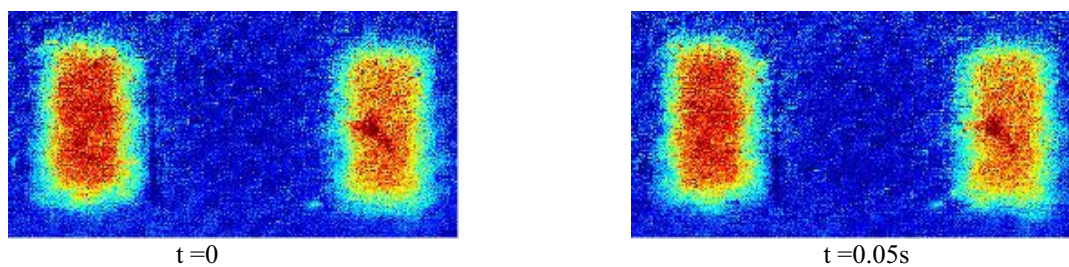


**Figure C. 33:** Instantaneous flow visualisation of the normalised concentration of the secondary jet at  $x/D=0.5$ , at 0.05 second intervals and  $\lambda = 2.8$ ,  $\gamma=7.84$ ,  $\kappa=4.7$ .



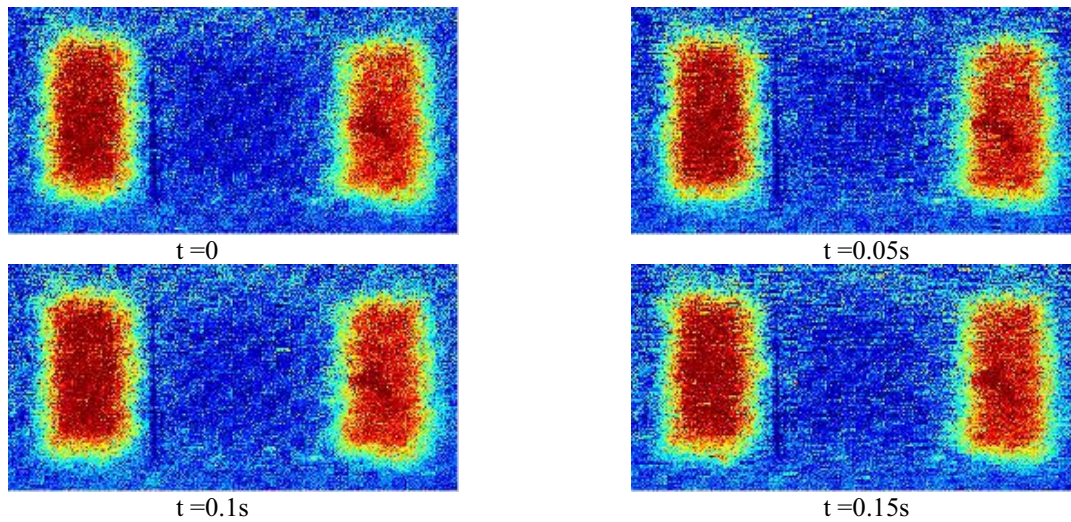


**Figure C. 34:** Instantaneous flow visualisation of the normalised concentration of the secondary jet at  $x/D=0.5$ , at 0.05 second intervals and  $\lambda = 3.6$ ,  $\gamma=12.96$ ,  $\kappa=7.78$ .

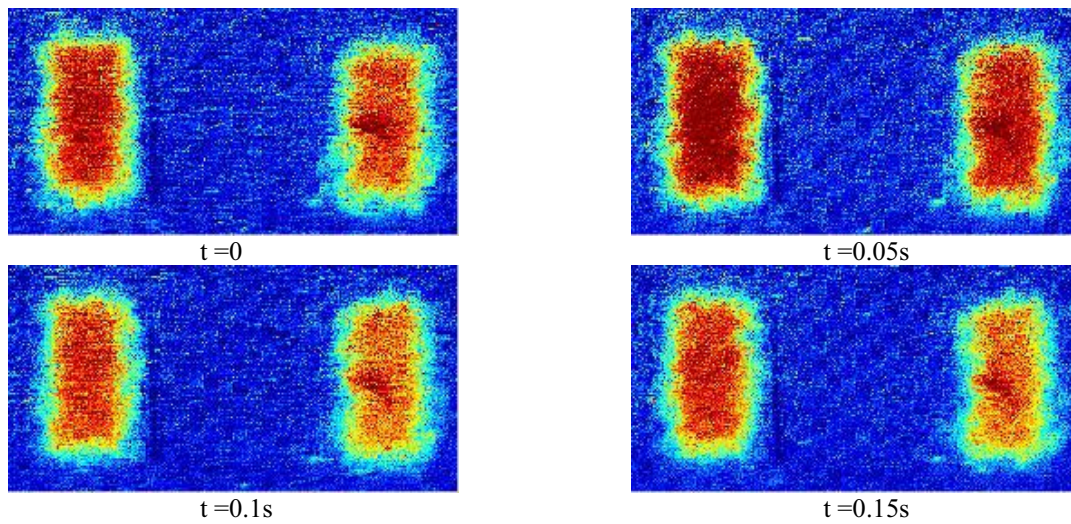


**Figure C. 35:** Instantaneous flow visualisation of the normalised concentration of the secondary jet at  $x/D=0.5$ , at 0.05 second intervals,  $\lambda = \infty$ ,  $x/D=0.5$ .

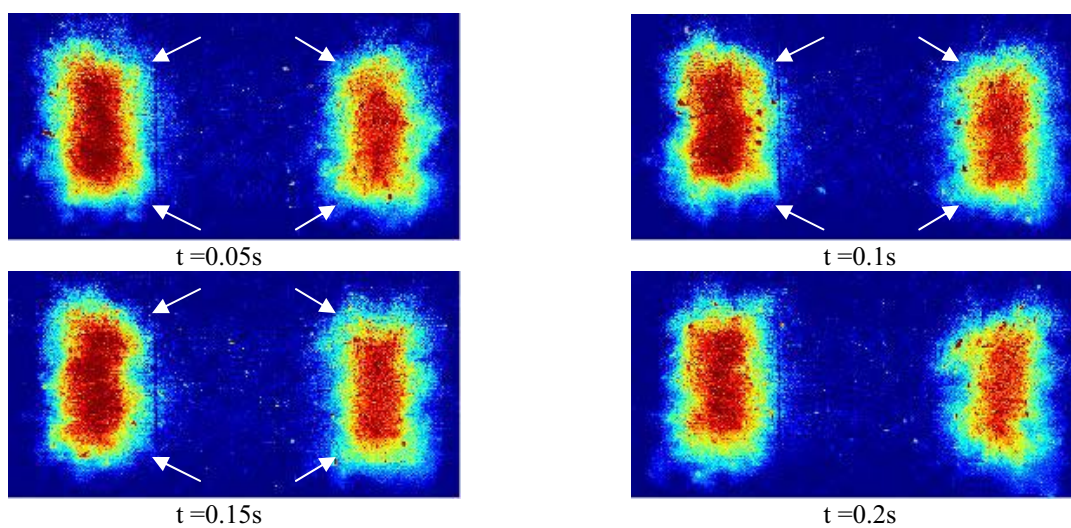


**Figure C. 36:** Instantaneous flow visualisation of the normalised concentration of the secondary jet at  $x/D=1$ , at 0.05 second intervals and  $\lambda = 0.55$ ,  $\gamma=0.3$ ,  $\kappa=0.18$ . The white arrows highlight the distortion of the secondary jets with an alteration in the local velocity gradients.



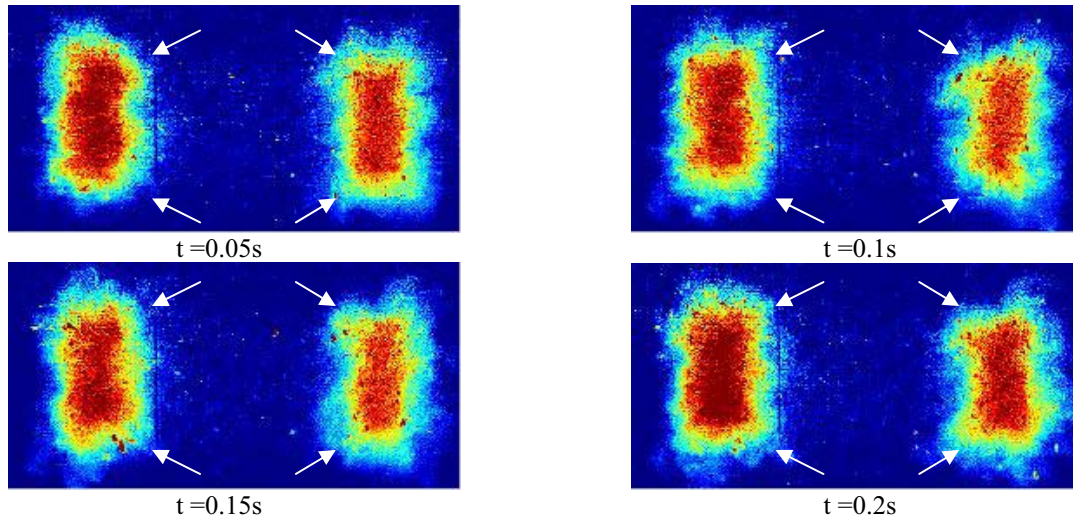


**Figure C. 37:** Instantaneous flow visualisation of the normalised concentration of the secondary jet at  $x/D=1$ , at 0.05 second intervals and  $\lambda = 1.4$ ,  $\gamma=1.96$ ,  $\kappa =4.7$ . The white arrows highlight the distortion of the secondary jets with an alteration in the local velocity gradients.

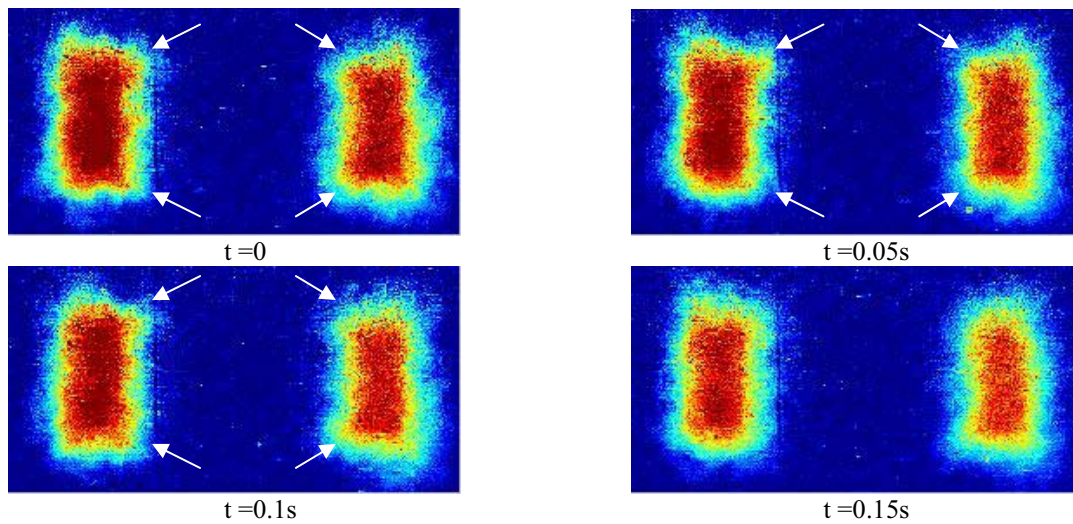


**Figure C. 38:** Instantaneous flow visualisation of the normalised concentration of the secondary jet at  $x/D=1$ , at 0.05 second intervals and  $\lambda = 2.8$ ,  $\gamma=7.84$ ,  $\kappa =4.7$ . The white arrows highlight the distortion of the secondary jets with an alteration in the local velocity gradients.

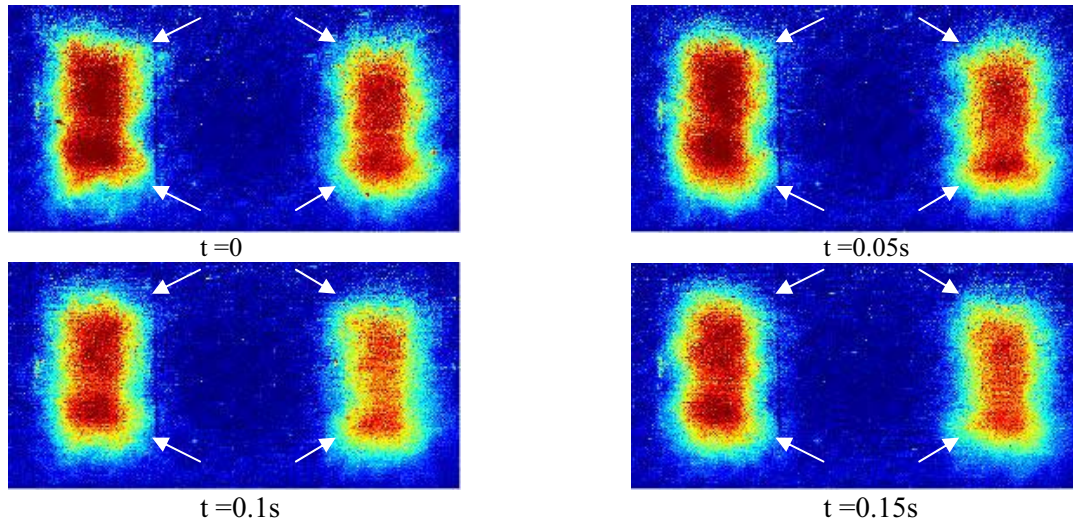


**Figure C. 39:** Instantaneous flow visualisation of the normalised concentration of the secondary jet at  $x/D=1$ , at 0.05 second intervals and  $\lambda = 3.6$ ,  $\gamma=12.96$ ,  $\kappa =7.78$ . The white arrows highlight the distortion of the secondary jets with an alteration in the local velocity gradients.

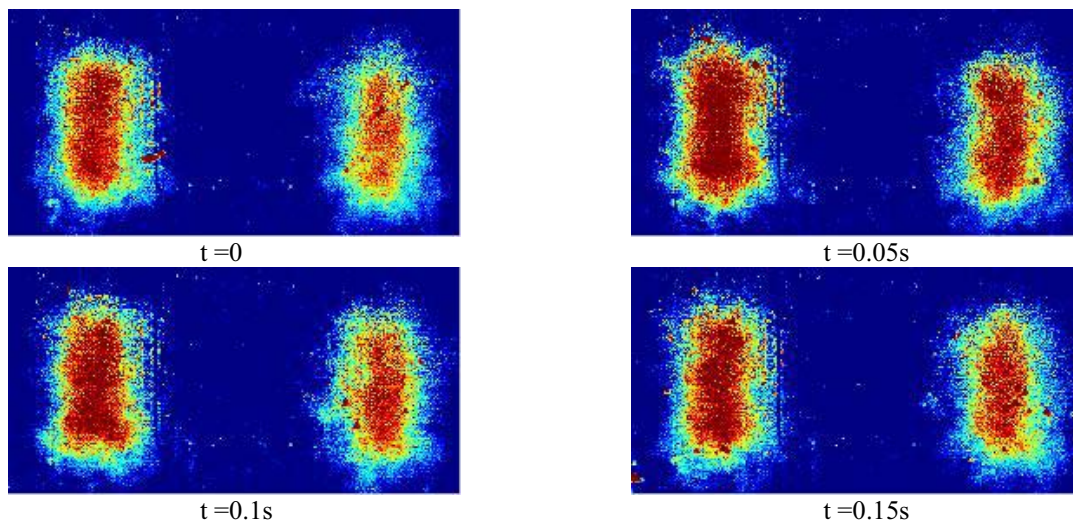


**Figure C. 40:** Instantaneous flow visualisation of the normalised concentration of the secondary jet at  $x/D=1$ , at 0.05 second intervals and  $\lambda = \infty$ .



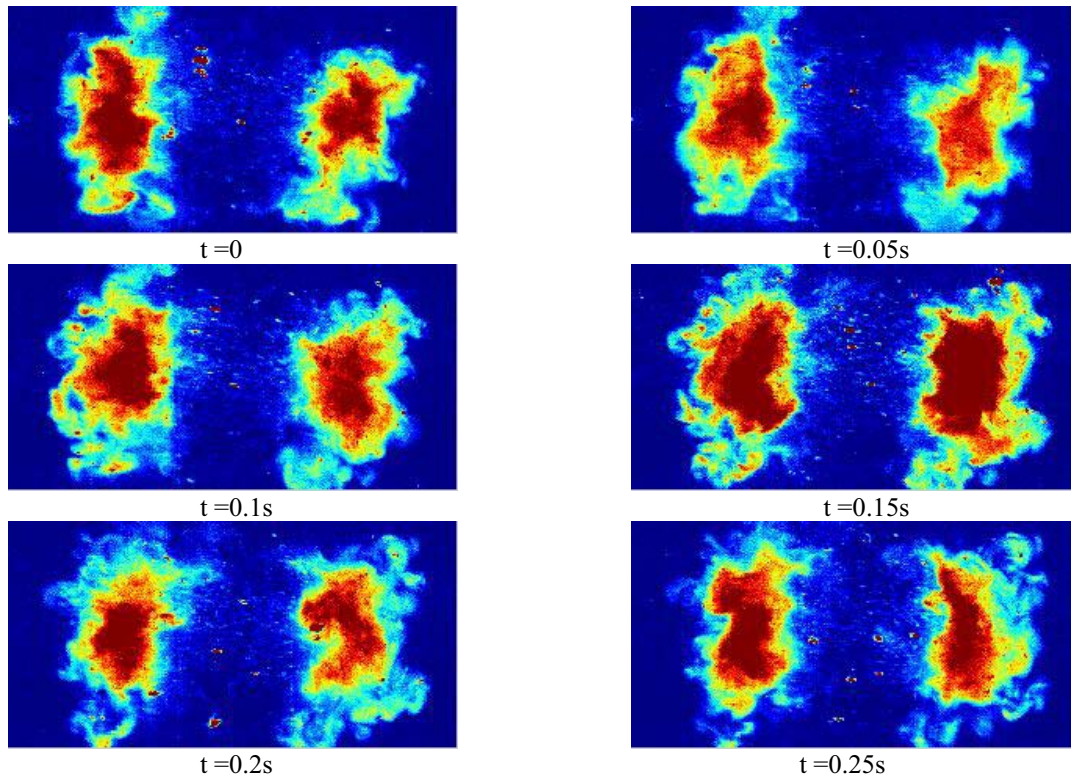


**Figure C. 41:** Instantaneous flow visualisation of the normalised concentration of the secondary jet at 0.05 second intervals and  $\lambda = 0.55$ ,  $\gamma = 0.3$ ,  $\kappa = 0.18$ ,  $x/D = 2$ .

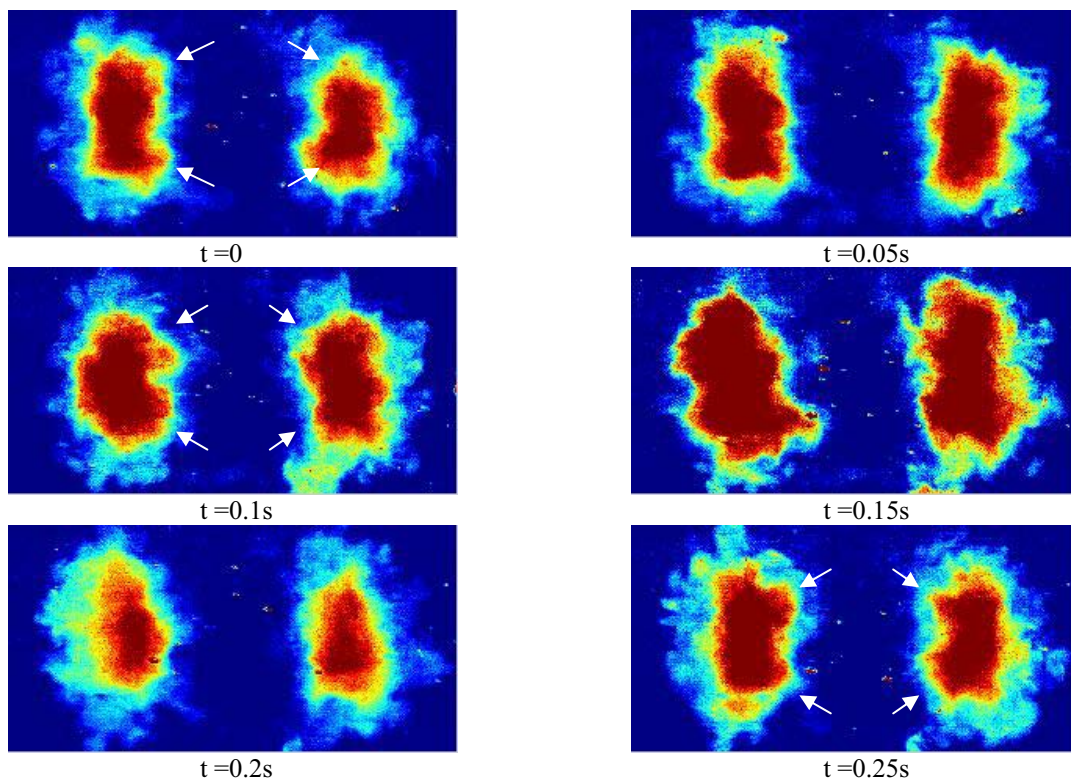


**Figure C. 42:** Instantaneous flow visualisation of the normalised concentration of the secondary jet at 0.05 second intervals and  $\lambda = 1.4$ ,  $\gamma = 1.96$ ,  $\kappa = 1.18$ ,  $x/D = 2$ . The white arrows highlight the distortion of the secondary jets with an alteration in the local velocity gradients.

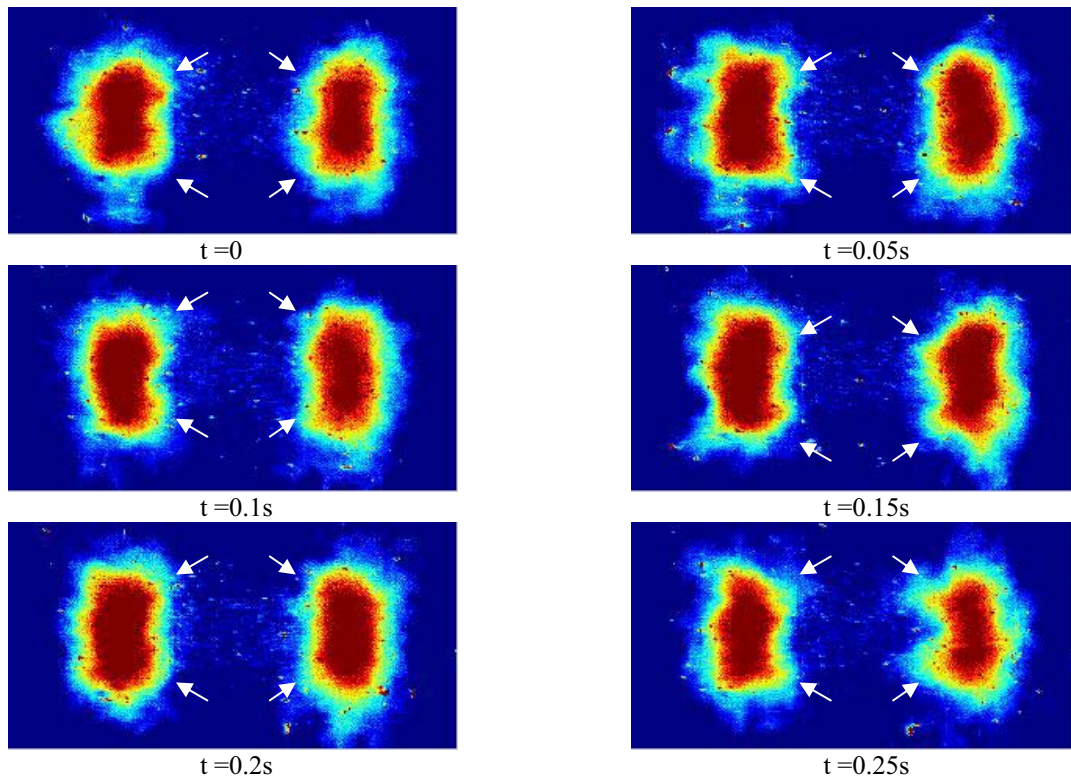


**Figure C. 43:** Instantaneous flow visualisation of the normalised concentration of the secondary jet at 0.05 second intervals and  $\lambda = 2.8$ ,  $\gamma = 7.84$ ,  $\kappa = 4.7$ ,  $x/D = 2$ . The white arrows highlight the distortion of the secondary jets with an alteration in the local velocity gradients.

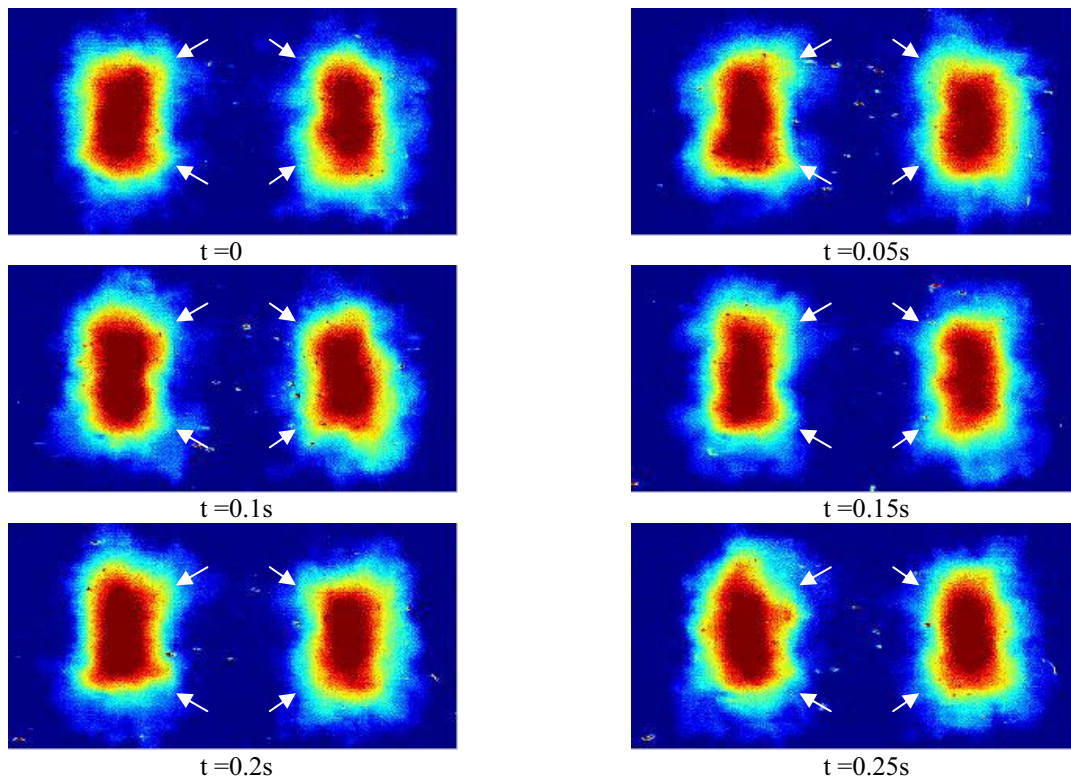


**Figure C. 44:** Instantaneous flow visualisation of the normalised concentration of the secondary jet at 0.05 second intervals and  $\lambda = 3.6$ ,  $\gamma = 12.96$ ,  $\kappa = 7.78$ ,  $x/D = 2$ . The white arrows highlight the distortion of the secondary jets with an alteration in the local velocity gradients.



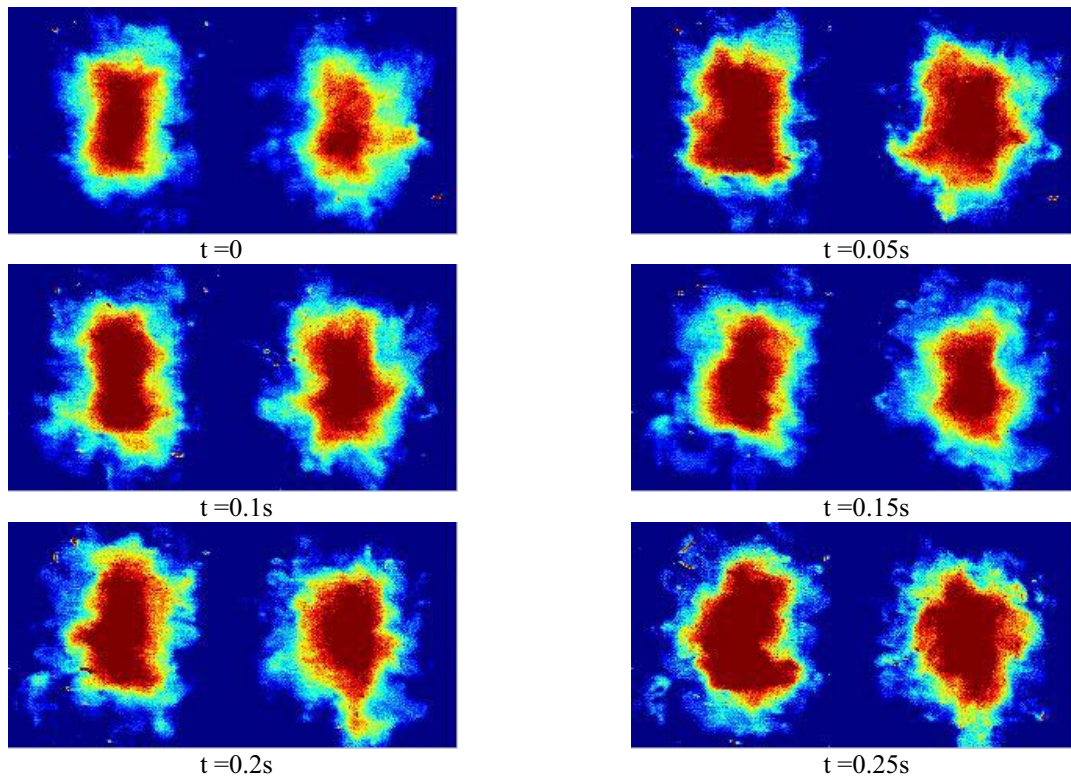


**Figure C. 45:** Instantaneous flow visualisation of the normalised concentration of the secondary jet at 0.05 second intervals and  $\lambda = \infty$ ,  $x/D = 2$ .

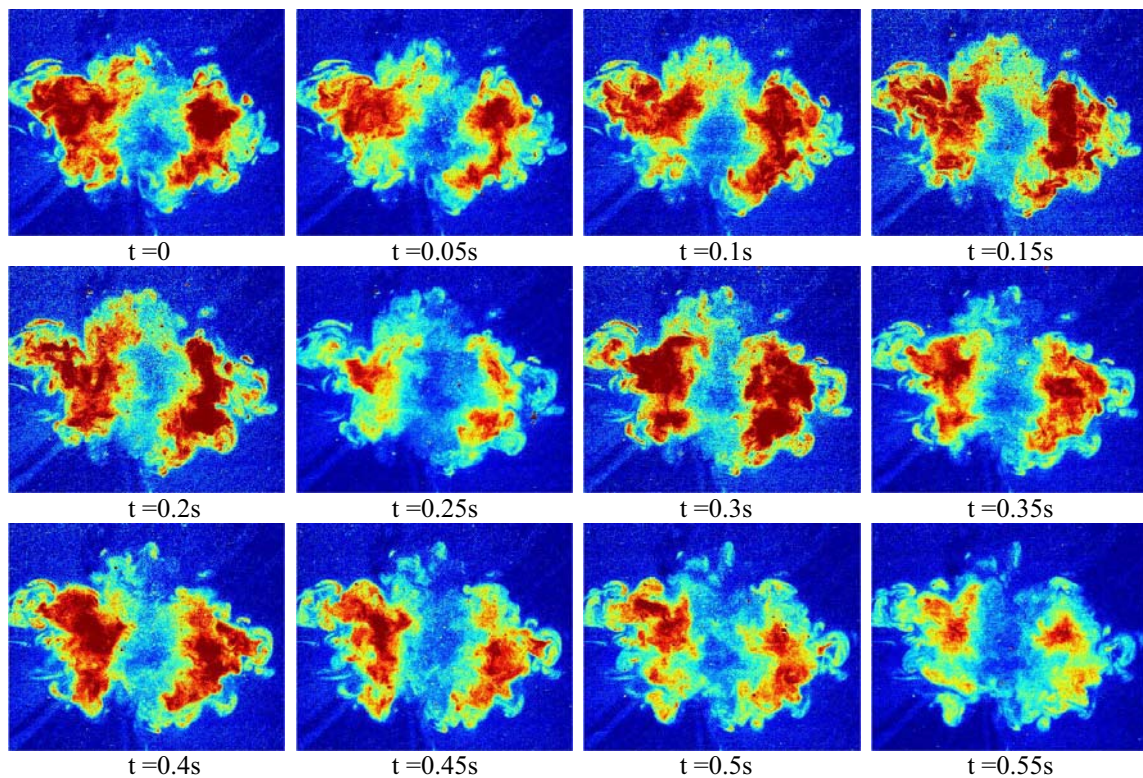


**Figure C. 46:** Instantaneous flow visualisation of the normalised concentration of the secondary jet at 0.05 second intervals and  $\lambda = 0.55$ ,  $\gamma = 0.3$ ,  $\kappa = 0.18$ ,  $x/D = 4$ .



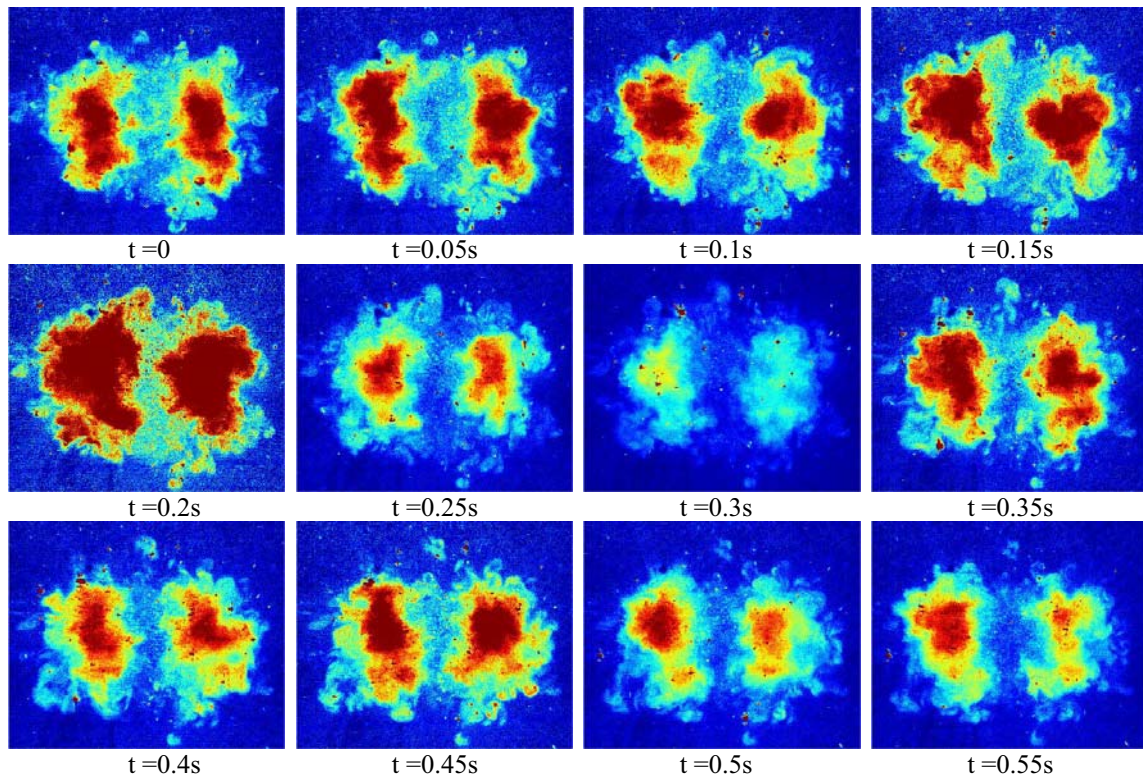


**Figure C. 47:** Instantaneous flow visualisation of the normalised concentration of the secondary jet at 0.05 second intervals and  $\lambda = 1.4$ ,  $\gamma = 1.96$ ,  $\kappa = 1.18$ ,  $x/D = 4$ .

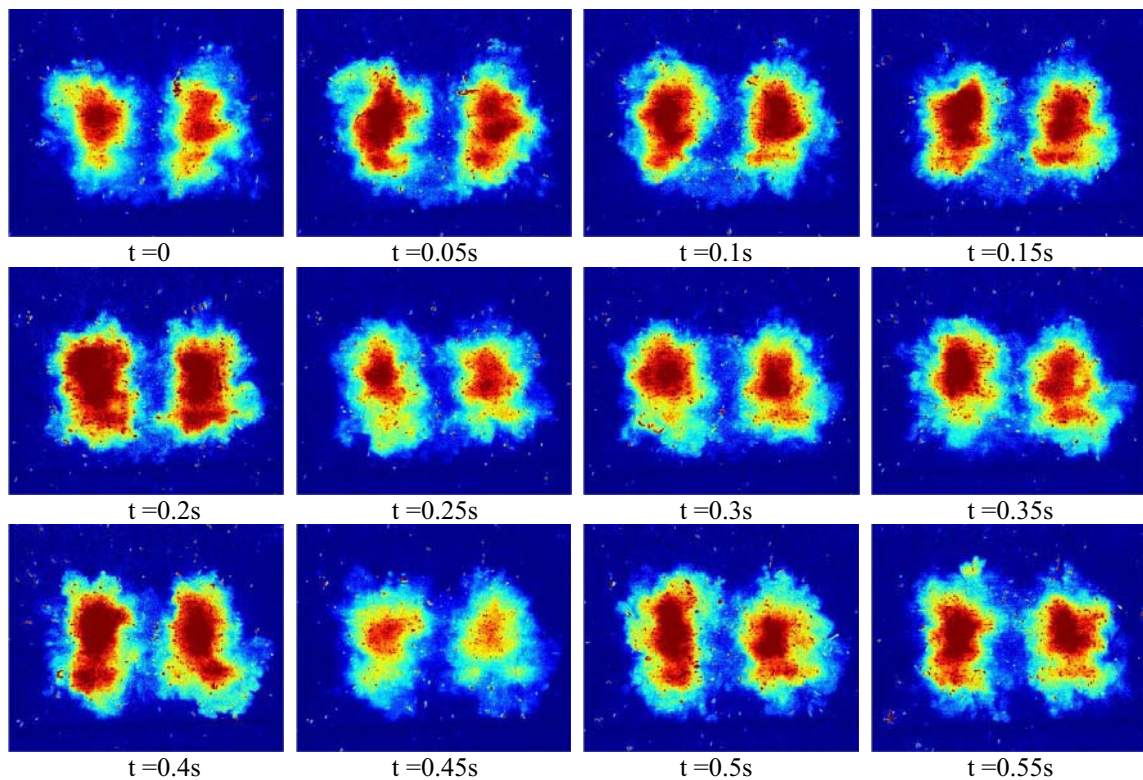


**Figure C. 48:** Instantaneous flow visualisation of the normalised concentration of the secondary jet at 0.05 second intervals and  $\lambda = 2.8$ ,  $\gamma = 7.84$ ,  $\kappa = 7.78$ ,  $x/D = 4$ .



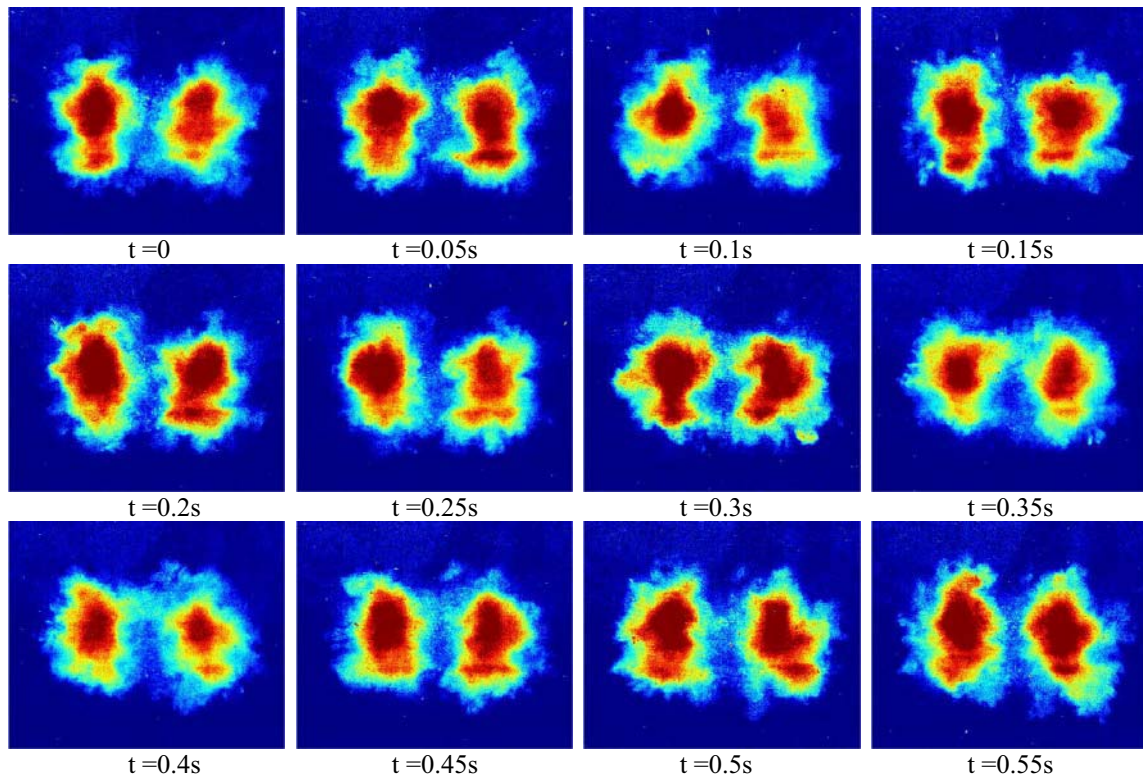


**Figure C. 49:** Instantaneous flow visualisation of the normalised concentration of the secondary jet at 0.05 second intervals and  $\lambda=3.6$ ,  $\gamma=12.96$ ,  $\kappa=7.78$ ,  $x/D=4$

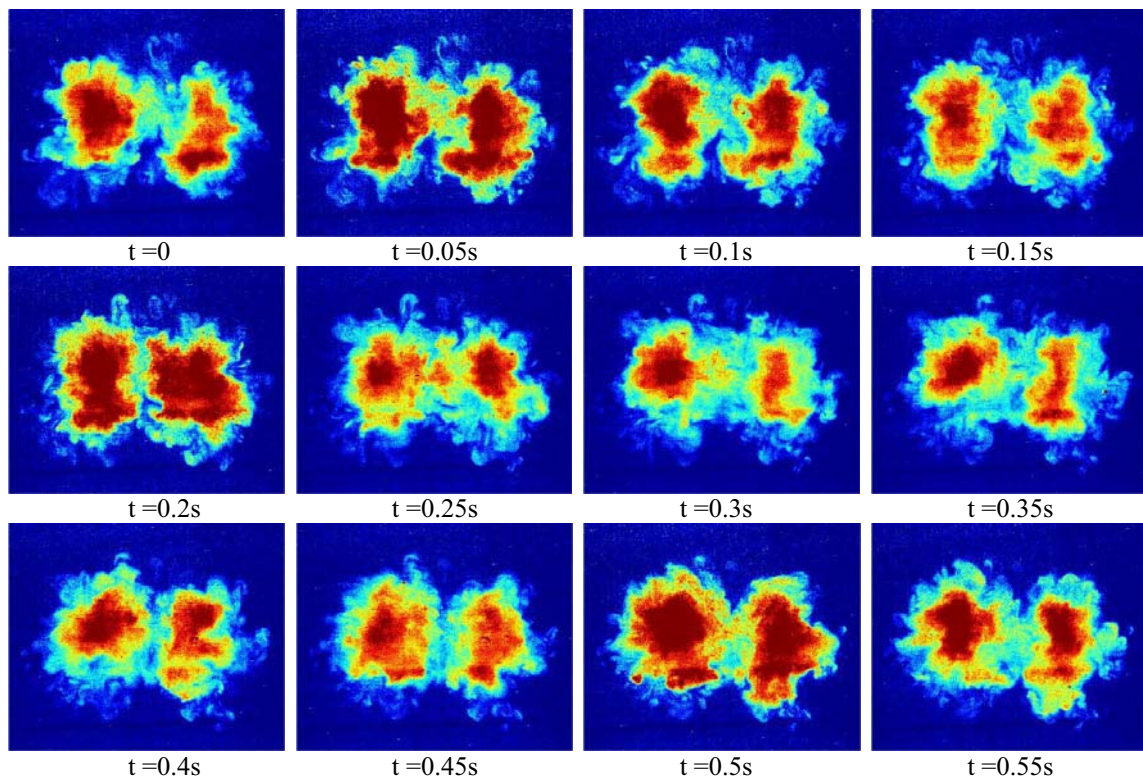


**Figure C. 50:** Instantaneous flow visualisation of the normalised concentration of the secondary jet at 0.05 second intervals and  $\lambda=\infty$ ,  $x/D=4$



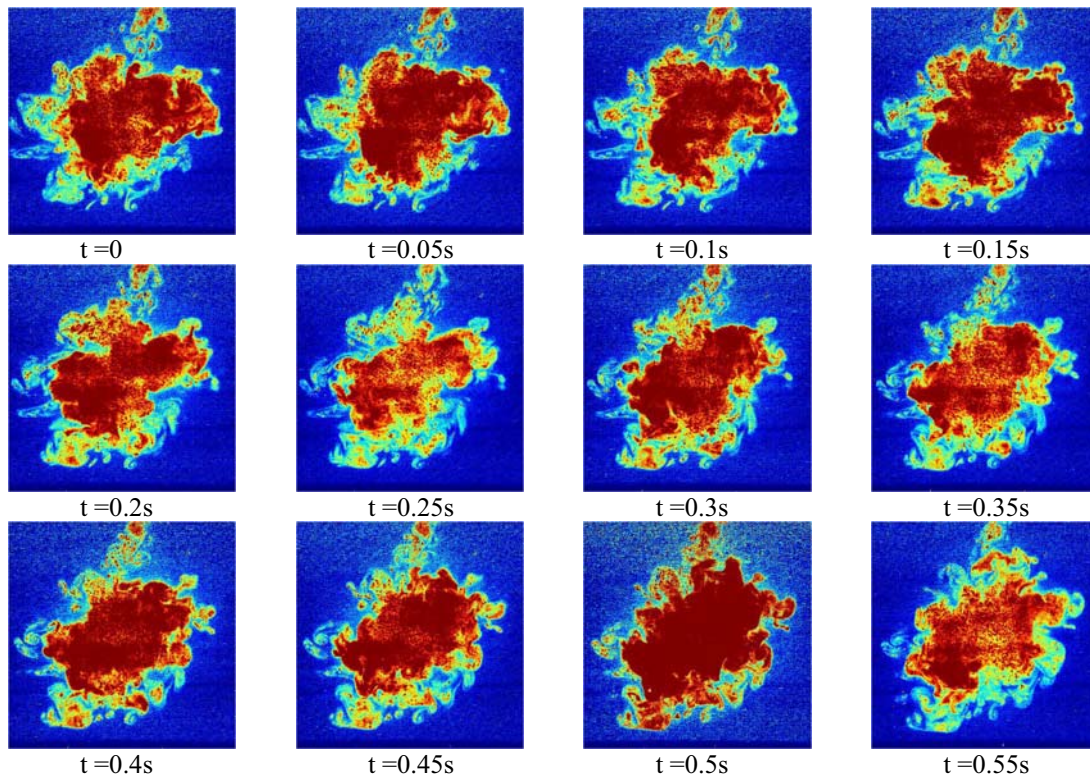


**Figure C. 51:** Instantaneous flow visualisation of the normalised concentration of the secondary jet at 0.05 second intervals and  $\lambda=0.55$ ,  $\gamma=0.3$ ,  $\kappa=0.18$ ,  $x/D=6$ .

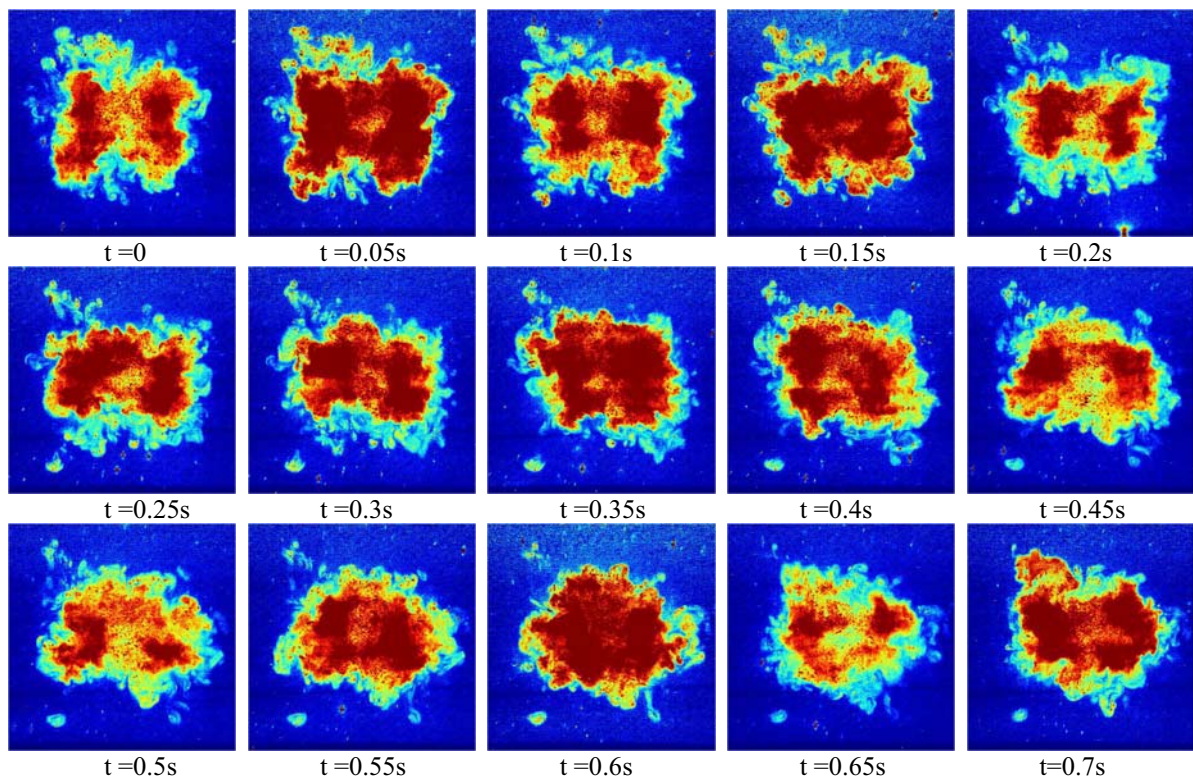


**Figure C. 52:** Instantaneous flow visualisation of the normalised concentration of the secondary jet at 0.05 second intervals and  $\lambda=1.4$ ,  $\gamma=1.96$ ,  $\kappa=1.18$ ,  $x/D=6$ .



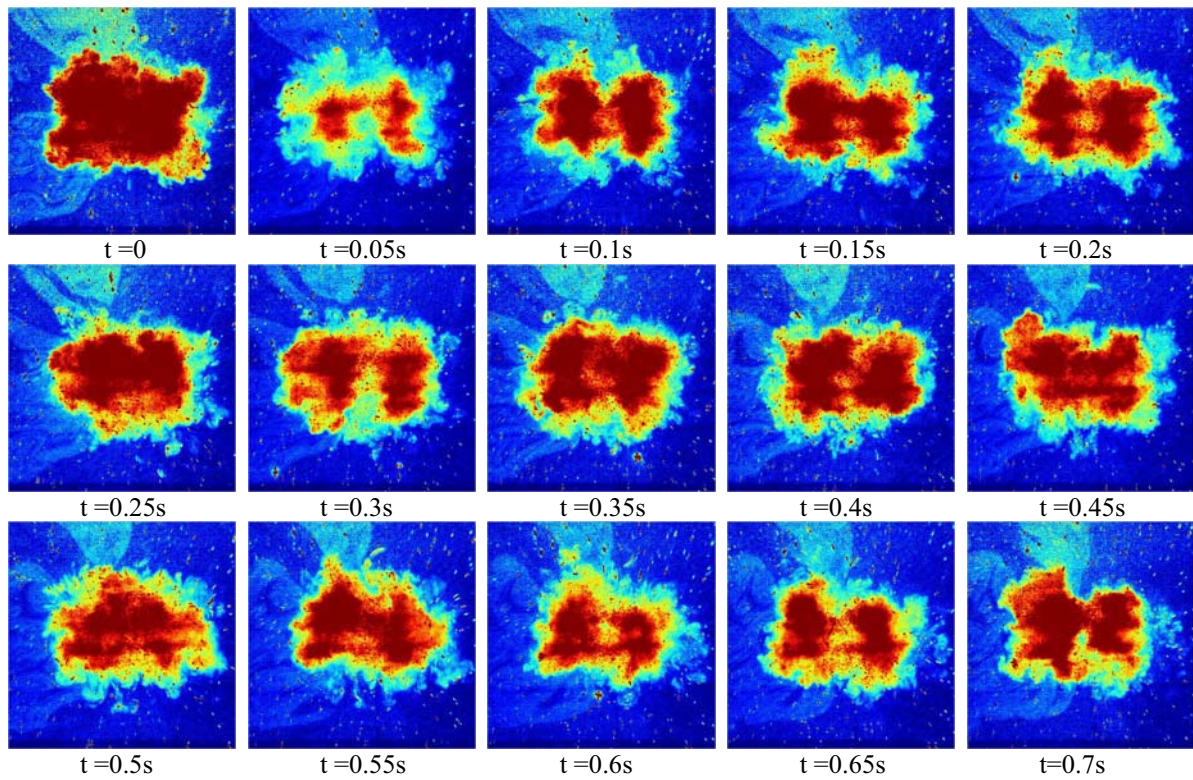


**Figure C. 53:** Instantaneous flow visualisation of the normalised concentration of the secondary jet at 0.05 second intervals and  $\lambda=2.8$ ,  $\gamma=7.84$ ,  $\kappa=4.7$ ,  $x/D=6$ .

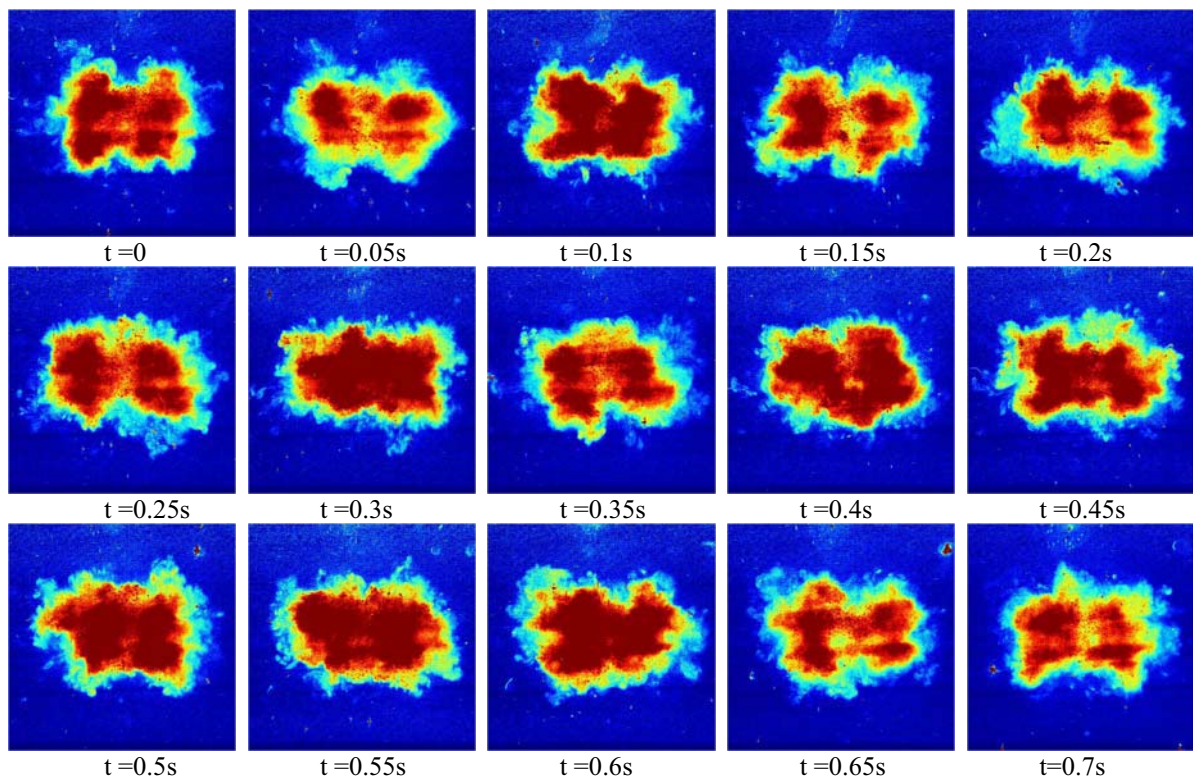


**Figure C. 54:** Instantaneous flow visualisation of the normalised concentration of the secondary jet at 0.05 second intervals and  $\lambda=3.6$ ,  $\gamma=12.96$ ,  $\kappa=7.78$ ,  $x/D=6$ .



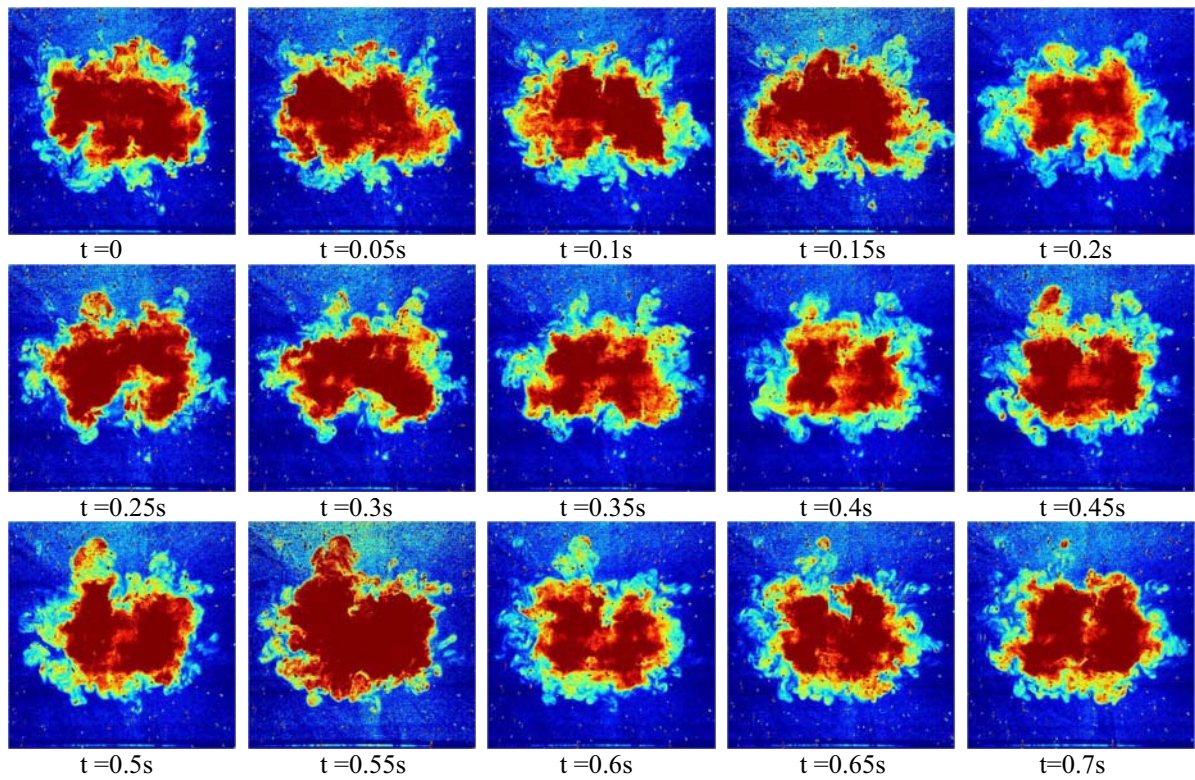


**Figure C. 55:** Instantaneous flow visualisation of the normalised concentration of the secondary jet at 0.05 second intervals and  $\lambda = \infty$ ,  $x/D=6$ .

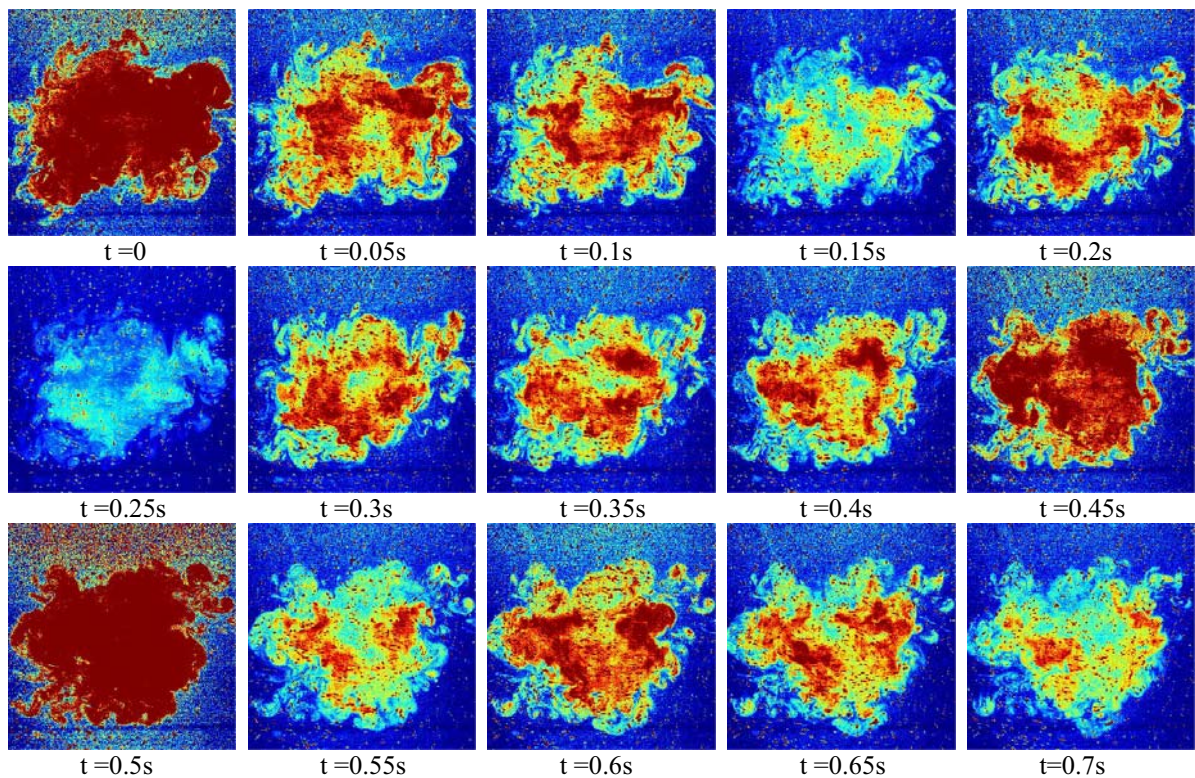


**Figure C. 56:** Instantaneous flow visualisation of the normalised concentration of the secondary jet at 0.05 second intervals and  $\lambda = 0.55$ ,  $\gamma = 0.3$ ,  $\kappa = 0.18$ ,  $x/D=8$ .



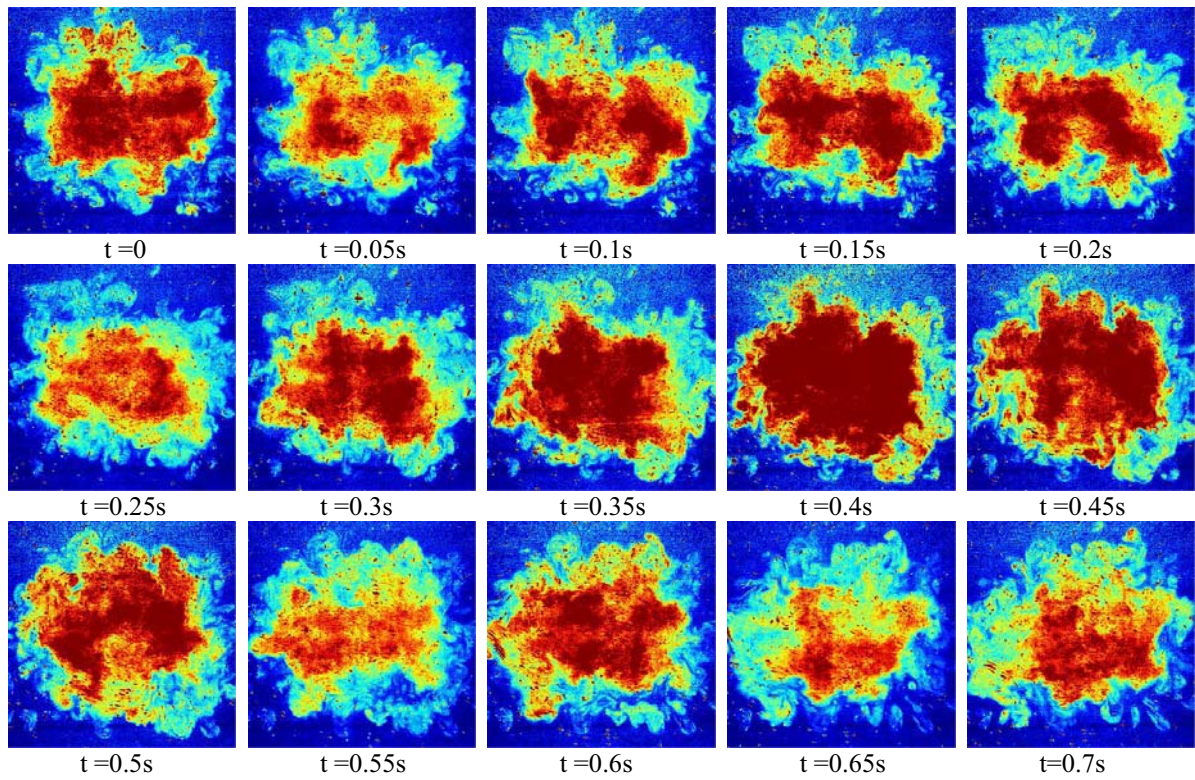


**Figure C. 57:** Instantaneous flow visualisation of the normalised concentration of the secondary jet at 0.05 second intervals and  $\lambda=1.4$ ,  $\gamma=1.96$ ,  $\kappa=1.18$ ,  $x/D=8$ .

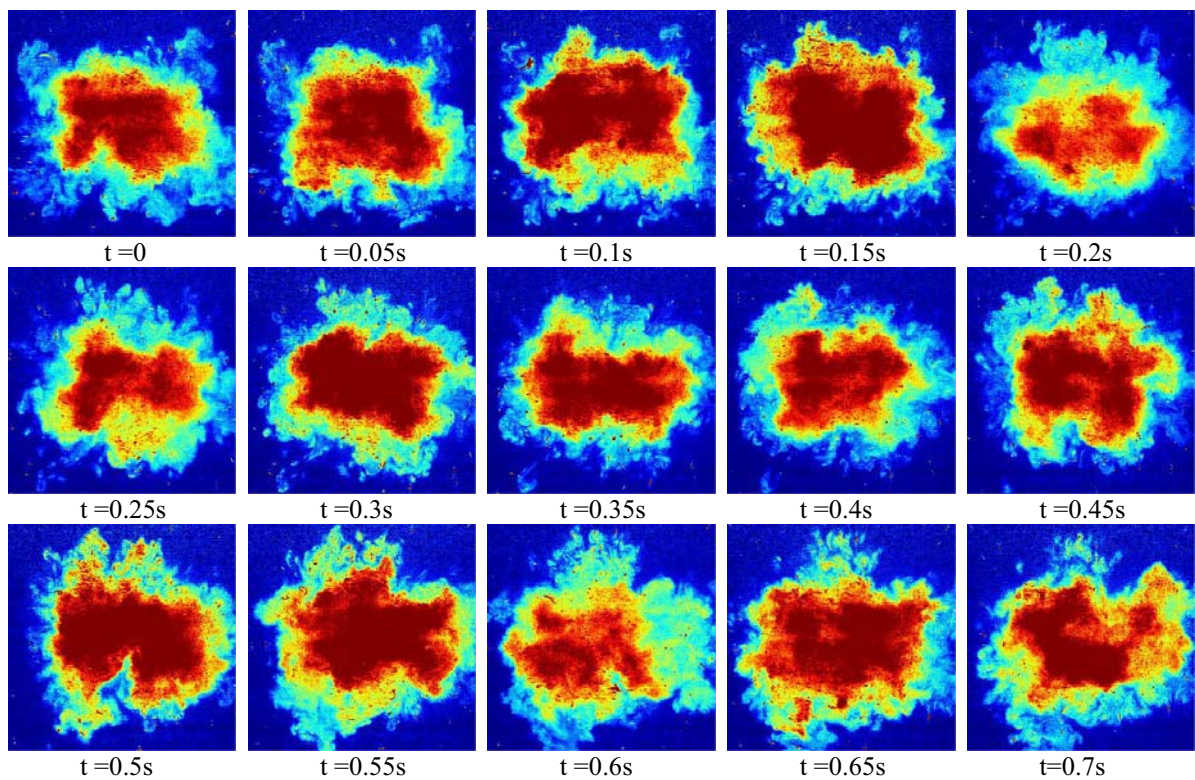


**Figure C. 58:** Instantaneous flow visualisation of the normalised concentration of the secondary jet at 0.05 second intervals and  $\lambda=2.8$ ,  $\gamma=7.84$ ,  $\kappa=4.7$ ,  $x/D=8$ .



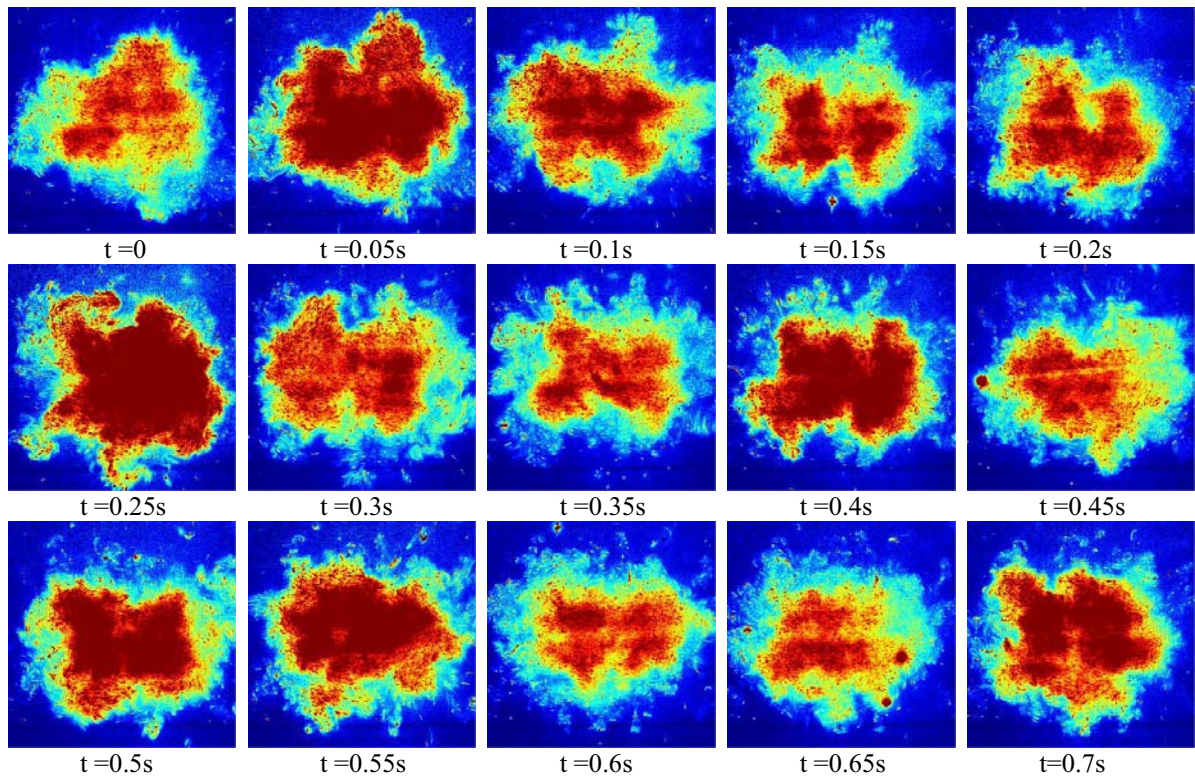


**Figure C. 59:** Instantaneous flow visualisation of the normalised concentration of the secondary jet at 0.05 second intervals and  $\lambda = 3.6$ ,  $\gamma = 12.96$ ,  $\kappa = 7.78$ ,  $x/D = 8$ .

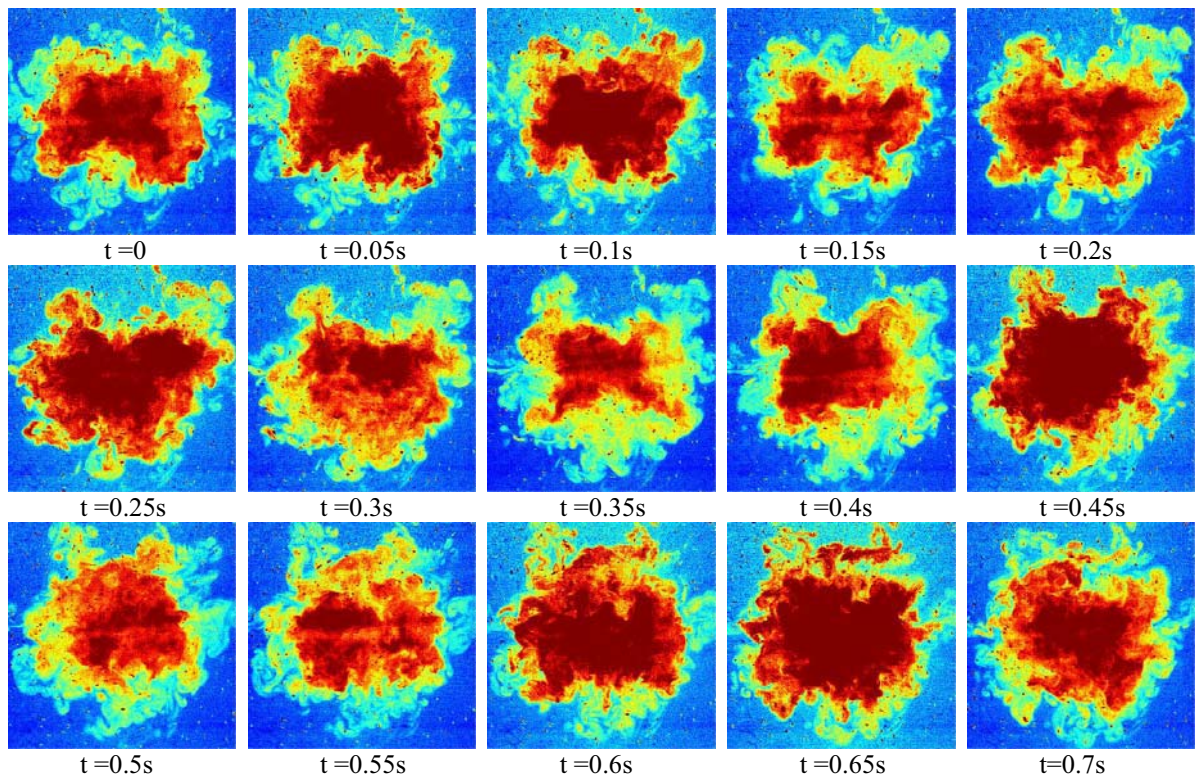


**Figure C. 60:** Instantaneous flow visualisation of the normalised concentration of the secondary jet at 0.05 second intervals and  $\lambda = \infty$ ,  $x/D = 8$ .